Agreement between Histomorphometry and Microcomputed Tomography to Assess Bone Microarchitecture of Dental Implant Sites

Danilo Rocha Dias, DDS, MS;* Cláudio Rodrigues Leles, DDS, MS, PhD;†
Aline Carvalho Batista, DDS, MS, PhD;‡ Christina Lindh, DDS, PhD;§
Rejane Faria Ribeiro-Rotta, DDS, MS, PhD‡

ABSTRACT

Background: Histomorphometry and microcomputed tomography (microCT) have been used in implant studies but need better understanding before being used as equivalent methods.

Purpose: The purpose of this study was to investigate the agreement between 2D (histomorphometry) and 3D (microCT) reference methods for assessing jawbone microarchitecture in vivo.

Material and Methods: Forty-four bone specimens from 32 patients were obtained during implant placement and examined by microCT, followed by hematoxylin–eosin staining and histomorphometric analysis. The morphometric parameters included bone volume density (BV/TV), bone surface fraction (BS/TV), bone surface density, trabecular thickness, trabecular number, and trabecular separation (Tb.Sp). Bland–Altman plots were used for pairwise agreement analysis between the equivalent 3D and 2D parameters, and complemented with Mountain plots. The association between the two methods was tested using Pearson's correlation followed by Passing–Bablok regression.

Results: Systematic bias was observed in all Bland–Altman and Mountain plots, including constant bias for BV/TV and Tb.Sp, and proportional bias for all other parameters. Significant correlation was found for BV/TV ($r = 0.80$; $p < .001$) and BS/TV ($r = 0.44$; $p = .003$), and the Passing–Bablok regression showed constant bias for BV/TV and proportional bias for BS/TV.

Conclusion: Because of the poor agreement between measures obtained by histomorphometry and microCT, these methods should not be used interchangeably for jawbones.

KEY WORDS: bone, computerized tomography, histological analysis, implant

INTRODUCTION

As trabecular bone tissue can be considered the most important in the peri-implant healing phase,[1] knowledge of trabecular bone microarchitecture is important for understanding its mechanical competence[2–4] and influence on the outcome of dental implant therapy.[5,6] Assessment of bone microarchitecture of human maxilla and mandible in vivo may help us to understand its influence on bone strength and whether or not it can affect changing on implant-bone interface after loading.[7,8] Furthermore, bone tissue microarchitecture is one parameter influencing "bone quality," in itself a concept of debate but still said to

*PhD student, Department of Oral Medicine, School of Dentistry, Federal University of Goias, Goiania, Goias, Brazil; †associate professor, Department of Prevention and Oral Rehabilitation, School of Dentistry, Federal University of Goias, Goiania, Goias, Brazil; ‡associate professor, Department of Oral Medicine, School of Dentistry, Federal University of Goias, Goiania, Goias, Brazil; §professor and head, Department of Oral and Maxillofacial Radiology, Faculty of Odontology, Malmö University, Malmö, Sweden

Reprint requests: Prof. Rejane Faria Ribeiro-Rotta, Department of Oral Medicine, School of Dentistry, Federal University of Goias, Rua C-235, N. 1323/1501 Nova Suíça Goiânia-GO 74280-130 Brazil; e-mail: rejanefrr@gmail.com

DOI 10.1111/cid.12176

be related to clinical results of implant stability and implant survival.[5,9–11]

Histomorphometry has been considered the standard reference method for bone microarchitecture analysis.[12–14] This method allows for assessment in two dimensions (2D) and provides an image with high spatial resolution and high contrast, but it is very time consuming.[13] A third dimension can only be added on the basis of stereology.[15] Measurement performed in histomorphometric analysis can be influenced by the selection of the section plane.[16] As another limitation, histomorphometry is destructive and does not allow for secondary measurements of a sample.[3,13] Microcomputed tomography (microCT) has been suggested as another standard reference method because of its high resolution and accuracy for both the 2D and three-dimensional (3D) study of bone structure, and because it is faster than histomorphometry.[13,17] Even though the use of microCT to study microarchitectural characteristics of jawbone tissue is relatively new, it provides the advantage of sample reusing.[6–8,18,19]

Validation of microCT as a reference method for bone morphometric evaluation has been reported, comparing it with the stereology-based histomorphometry, which still remains the "gold standard."[13,14,20] Studies have been performed in animal bone,[21–25] human cadavers,[13] and in vivo human bone,[14,20,26–29] but not in jawbone. Therefore, the aim of this study was to evaluate the agreement between microCT (3D) and histomorphometry (2D) in in vivo human jawbone.

MATERIAL AND METHODS

Sample

This was a cross-sectional observational study approved by the Ethics Committee of the Federal University of Goias, Brazil (protocol n. 114/2007), and all volunteers agreed to participate by signing the term of consent. Thirty-two volunteers were selected after clinical examination and fulfilled the following inclusion criteria: partial edentulousness with dental implant treatment indication and estimated amount of alveolar bone considered enough by clinical and imaging evaluation (periapical, panoramic, and computed tomography). Exclusion criteria included no complex oral rehabilitations needs, no metabolic diseases or allergies, smoke free for at least 10 years, and good oral hygiene care.

Bone Biopsies

Bone biopsies were performed under local anesthesia prior to implant installation with a 2.7 mm inner diameter trephine specifically designed for this study. The specimens were maintained in a buffered 10% formalin solution. The implant placement followed the traditional two-stage surgical protocol,[30] and prosthetic rehabilitation was performed after osseointegration.

MicroCT

MicroCT of the bone biopsies were performed using Skyscan 1172 equipment (Antwerp, Belgium) with the following technical parameters: 120 mA and 92 kV power intensity, aluminum filter and 180° rotation, and pixel size or resolution for acquisition, and image reconstruction of 2.7 μm. The data scanned by the capture card was sent to the computer using tomographic reconstruction software NRecon version 1.4.4 (Skyscan, Antwerp, Belgium). The reconstructed images were reformatted as 3D images and analyzed by CT-An software (CTAnalyser, Skyscan, Antwerp, Belgium), which calculated the 3D morphometric parameters of the bone in each volume of interest (VOI).

Histomorphometry

After microCT analysis, the specimens were demineralized in an EDTA solution (pH 7.0) for 1 week, automatically processed (OMA DM-20, M20090257, Sao Paulo, Brazil), embedded in paraffin, sectioned longitudinally with a microtome (Leica RM2165, Merck KGaA, Darmstadt, Germany) in 5 μm slices, and stained using routine hematoxylin/eosin techniques. The most central section was selected to perform the histomorphometric measurements. It should correspond to the greatest dimensions of the specimen in length and diameter. Digital microscopic images were obtained using a digital camera connected to an optical microscope (×5; Axio Scope A1 and Axiocam ERc 5 s, Carl Zeiss, Göttingen, Germany), which had been previously calibrated. An average of two microscopic fields were analyzed from each bone specimen. Measurements of total bone perimeter length (P_B), total bone area (A_B), and total section area (A_T) were performed using the AxioVision Release 4.7 microscope software (Carl Zeiss) (Figure 1).

Morphometric Analysis

MicroCT provided measurements obtained directly from reconstructed images (CT-An analyzer, Skyscan)

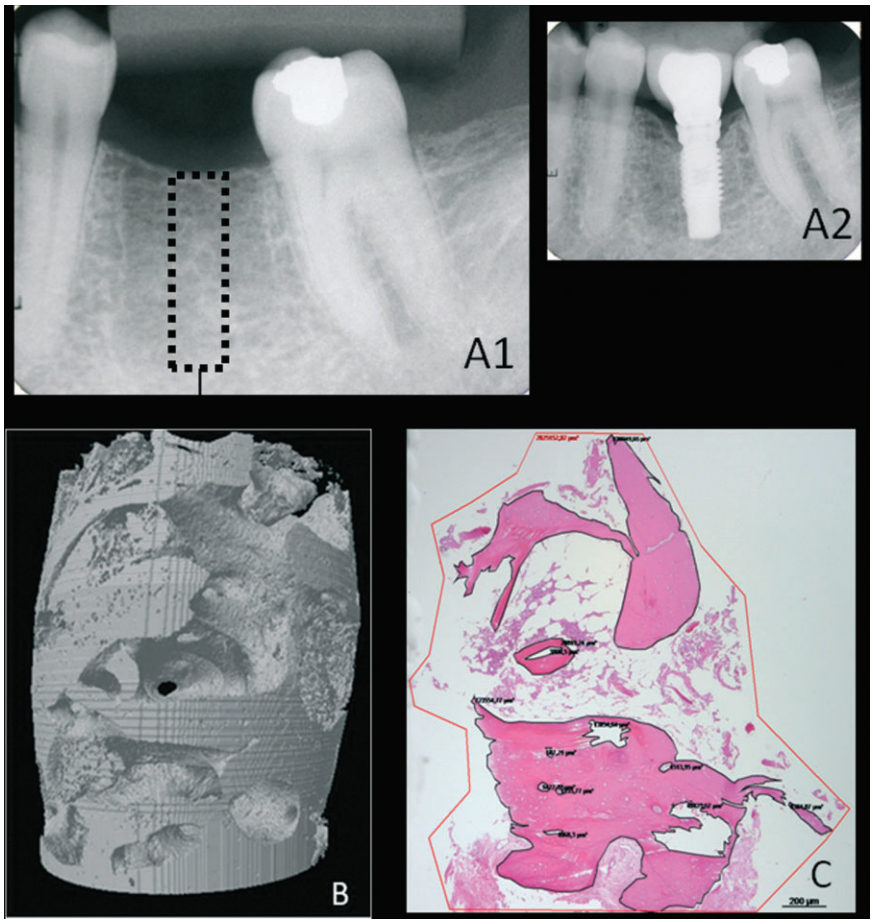

Figure 1 MicroCT 3D image reconstruction (B) and histological slice (C) of bone specimens (hematoxylin and eosin/original magnification × 5) obtained from lower first-molar area (A1) rehabilitated by prosthesis supported by osseointegrated implant (A2). Histomorphometric measurements (C) show the total bone area (trabecular bone) in black and total section area (trabecular bone + bone marrow) in red. Images obtained using Axiovision 4.7 software (182 × 66; 150 × 150 DPI).

(Figure 1) based on consecutive 2D images. Several measurements could be obtained from this method, including 3D primary measurements, which were described as tissue volume (TV), bone volume (BV), bone surface (BS), and trabecular thickness (Tb.Th), as well as other derived measurements. However, only those measurements that could be correlated with histomorphometric parameters were selected for this study. They included:

- *BV density* (BV/TV) was the ratio of the trabecular BV to the total TV of the VOI;
- *BS fraction* (BS/TV) was the ratio of the BS area to the total TV of the VOI;
- *BS density* (BS/BV) was a ratio of the BS area to the trabecular BV of the VOI;
- *Tb.Th* was calculated from the trabecular BV and the total TV;
- *Trabecular number* (Tb.N) was calculated from the reciprocal of the distance between the center and the center of trabeculae;
- *Trabecular separation* (Tb.Sp) was the distance between adjacent trabeculae.

The 3D microCT measurements, obtained by algorithms of computer graphics, are illustrated in Figure 2.

Using a calculation proposed by Parfitt and colleagues in 1983,[15] the primary 2D histomorphometric measurements (P_B, A_B, and A_T) allowed us to obtain estimated 3D parameters based on the stereology. Standardized nomenclature, symbols, and units[12] allowed for a comparison of the histomorphometric parameters to direct 3D measurements obtained by microCT analyses. The formulas and correspondence between these parameters are described in Table 1. The data

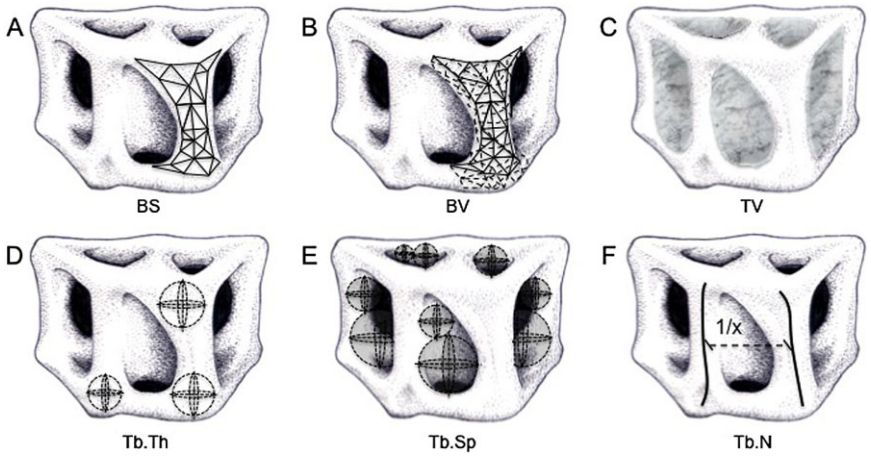

Figure 2 MicroCT measurements: All the 3D measurements were performed automatically by CT-An analyzer. They were based on the solid content and spaces of the volume of interest (VOI), using the algorithms of computer graphics (i.e., Marching Cubes method). The solid content enables the measurements of the bone surface (BS) from surface triangulation (A), the bone volume (BV) by defining tetrahedrons from the surface triangulated (B), and the trabecular thickness (Tb.Th) using spherical algorithms (D). The spaces allow measurements of trabecular separation (Tb.Sp), also using spherical algorithms (E). The total solid and spaces content are the tissue volume (TV), corresponding to the VOI (C). The trabecular number (Tb.N) was taken as the inverse of the mean distance between the mid-axes of the structure examined (F), implying the number of crossings through a trabecular or solid structure, done per unit length in a random linear path through the VOI.

were expressed as percentages and given in millimetres or micrometers.

Data Analysis

Descriptive analysis was expressed by data mean, standard deviation, range, and median values for both histomorphometry and microCT. Bland–Altman plots were generated to provide a graphical visualization of the agreement between the two measurement methods.[31] The mean values (*X*-axis) were plotted against the percent difference between the two methods (*Y*-axis) to identify any systematic bias and possible outliers. Horizontal lines were drawn at the mean difference and at the limits of agreement, defined as the mean difference plus and minus 1.96 times the standard deviation of the differences.

Additionally, the Mountain plot (also called "folded empirical cumulative distribution plot") was used as a complement to the Bland–Altman plots, which was created by calculating a percentile for each ranked difference between the two methods.[32] To get a folded plot, the following transformation was performed for all percentiles above 50: percentile = 100 – percentile. These percentiles were then plotted against the differences between the two methods. The Mountain plot provides information about the distribution of the differences

TABLE 1 System of Nomenclature, Symbols, and Units Suggested by Parfitt et al. (1987) and the Calculation Formulas of Morphometric Parameters That Allowed for Comparison between the 2D (Histomorphometry) and 3D (microCT) Methods

Parameter	Symbol	Unit	Formulas to Calculate 3D Parameters from Primary 2D Measurements	Formulas to Calculate 3D Parameters from Primary 3D Measurements
Bone volume density	BV/TV	%	$(A_B/A_T)100$	BV/TV
Bone surface fraction	BS/TV	mm^{-1}	$(P_B/A_T)1.199$	BS/TV
Bone surface density	BS/BV	mm^{-1}	$(P_B/A_B)1.199$	BS/BV
Trabecular thickness	Tb.Th	mm	$(2/1{,}199)(A_B/P_B)$	$2 \times BV/BS$
Trabecular number	Tb.N	mm^{-1}	$(1{,}199/2)(P_B/A_T)$	$BV/(TV \times Tb.Th)$
Trabecular separation	Tb.Sp	mm	$(2/1{,}199)(A_T - A_B)/P_B$	1/Tb.N – Tb.Th

A_B = bone area; A_T = total area; P_B = bone perimeter; BV = bone volume; BS = bone surface; TV = tissue volume.

TABLE 2 Descriptive Data of 2D (Histomorphometry) and 3D (MicroCT) Morphometric Parameters

Morphometric parameters	Units		Mean (SD)	Min–Max	Median
Bone volume density (BV/TV)	%	2D	51.69 (16.3)	17.69–82.92	52.34
		3D	34.97 (14.2)	11.09–67.95	33.1
Bone surface fraction (BS/TV)	mm^{-1}	2D	4.51 (1.28)	2.6–8.97	4.16
		3D	12.14 (8.11)	4.14–49.69	9.81
Bone surface density (BS/BV)	mm^{-1}	2D	10.16 (5.6)	3.71–27.57	8.79
		3D	40.37 (31.15)	7.45–143.89	31.86
Trabecular thickness (Tb.Th)	mm	2D	0.25 (0.12)	0.07–0.54	0.23
		3D	0.11 (0.07)	0.02–0.33	0.09
Trabecular number (Tb.N)	mm^{-1}	2D	2.25 (0.64)	1.3–4.48	2.08
		3D	4.45 (3.02)	0.85–14.96	3.66
Trabecular separation (Tb.Sp)	mm	2D	0.22 (0.08)	0.1–0.41	0.21
		3D	0.36 (0.1)	0.2–0.61	0.32

2D = two dimension; 3D = three dimension; microCT = microcomputed tomography; SD = standard deviation.

between the methods. If the histomorphometry and microCT methods are unbiased, then the mountain is centered over the zero line on the *X*-axis, and if a long tail on the curve is observed, this reflects large differences and systematic bias between the methods. MicroCT measurements were subtracted from the corresponding histomorphometric measurements in all Bland–Altman and Mountain plots.

Pearson's correlation analysis was performed to measure the degree of association between two variables. In the assumption of linear relationship and high correlation, a specific regression analysis was performed using the Passing–Bablok regression method. This analysis provides a linear regression with no special assumptions regarding the distribution of the samples, and the measurement errors do not depend on the assignment of a method to the *X*- and *Y*-axes.[33] The slope "*b*" of the regression line and the intercept "*a*" were calculated with their 95% confidence intervals (CIs). These CIs are used to determine whether there is only a chance difference between "*b*" and 1 (if "*b*" differs significantly from 1, there is at least a proportional difference between the two methods) and between "*a*" and 0 (if "*a*" differs significantly from 0, both methods differ at least by a constant bias). Interpretation of the results of the Passing–Bablok procedure supplemented the results of the Bland–Altman and Mountain plots.

RESULTS

A total of 44 specimens from 32 patients (18 women and 14 men, mean age: 42 years old) were analyzed. All specimens were 2.7 mm in diameter and 2.5 to 13.0 mm in length. Table 2 shows the descriptive data of histomorphometric and microCT parameters.

Table 3 shows the results of the relationships between data using linear regression, Bland–Altman, and Passing–Bablok regression for each corresponding microCT and histomorphometric parameters. Systematic bias was observed in all of the Bland–Altman plots, including constant bias for BV/TV and Tb.Sp, and proportional bias for all other parameters (BS/BV, BS/TV, Tb.Th, and Tb.N) (Figure 3).

Pearson's correlation analysis indentified two parameters for which the 2D and 3D measurements have a linear relationship and are significantly correlated. They were BV/TV ($r = 0.80$; $p < .001$) and BS/TV ($r = 0.44$; $p = .003$). The subsequent regression analysis for these two parameters using the Passing–Bablok method confirmed the results found using the Bland–Altman plots. From the analysis of intercept "*a*," the results revealed that the $a = 0$ hypothesis was rejected for BV/TV. This indicates that the 2D and 3D methods differ by at least a constant bias for this parameter. On the other hand, from the analysis of slope *b*, the hypothesis that $b = 1$ was rejected for BS/TV, which means that there is a proportional difference between the two methods (Table 3).

Figure 3 shows a panel of graphical methods, revealing for BV/TV a constant bias with limits of differences excluding the null difference line (Figure 3 panel A1), and a normal distribution of the dot plot, without the Mountain plot distribution centered over zero (Figure 3 panel B1). The graphs for BS/TV show the proportional bias

TABLE 3 Relationships between the Data Using Linear Regression (*r*), Bland–Altman Plots, and Passing–Bablok Regression

Morphometric Parameters (2D and 3D)	Bland–Altman Plots Bias % (95%CI)	*r* (*p* Value)	Passing–Bablok Regression	
			Intercept *a* (95%CI)	Slope *b* (95%CI)
BV/TV	40.9 (−8.1 to 90.0)	0.80 (<.001)	−9.87 (−20.0 to −1.12)	0.86 (0.68 to 1.09)
BS/BV	−108.1 (−31.8 to −184.4)	0.12 (.446)	–	–
BS/TV	−76.7 (10.8 to −164.2)	0.44 (.003)	−60.21 (−381.88 to −22.29)	17.03 (7.74 to 93.94)
Tb.Th	79.6 (−32.4 to 191.6)	0.21 (.170)	–	–
Tb.N	−44.7 (83.6 to −173.0)	−0.10 (.519)	–	–
Tb.Sp	−47.5 (25.6 to −120.5)	0.20 (.192)	–	–

2D = two dimension; 3D = three dimension; CI = confidence interval; BS/BV = bone surface density; BS/TV = bone surface fraction; BV/TV = bone volume density; Tb.N = trabecular number; Tb.Th = trabecular thickness.

between the methods (Figure 3 panel A2) and the skewness distribution and long tail of the Mountain plot (Figure 3 panel B2), reflecting the differences between the methods.

DISCUSSION

Although both histomorphometry and microCT are considered reference methods to assess bone tissue, this

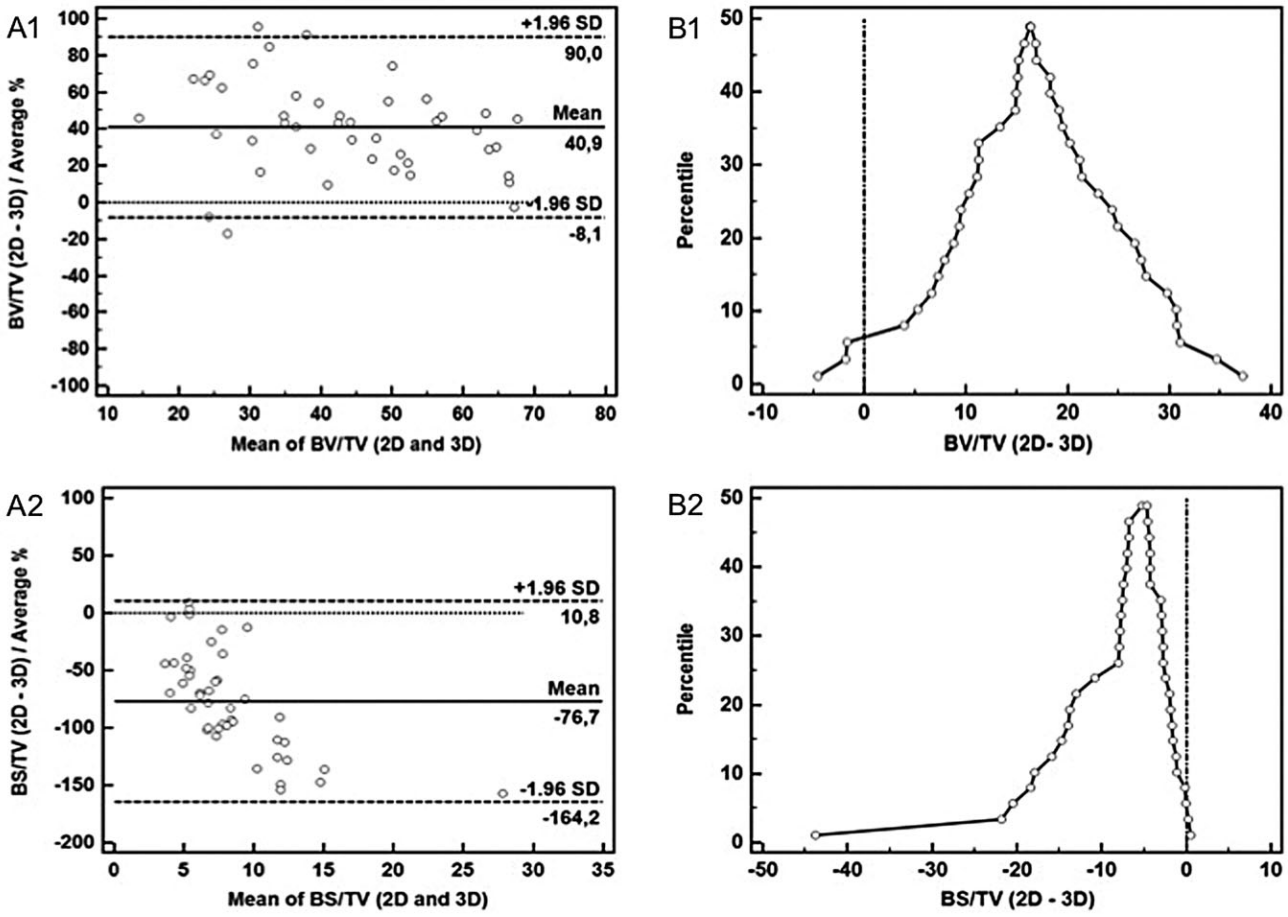

Figure 3 Bland–Altman plots comparing the agreement between histomorphometry (2D) and microcomputed tomography (microCT; 3D) for the following parameters: (A1) bone volume density (BV/TV) and (A2) bone surface fraction (BS/TV). Mountain Plots showing the distribution of the differences between the two methods for BV/TV (B1) and BS/TV (B2).

study showed that these methods should not be used interchangeably for jawbone microarchitecture evaluation, because systematic biases were found for all the evaluated morphometric parameters in the agreement analysis.

The findings of this study are difficult to compare with other reports, because no previous study assessed the agreement between microCT and histomorphometry for in vivo human jawbone sites. The majority of previous studies used different ranges of specimen dimensions and used samples from different anatomical regions, such as the iliac bone[13,14,20,26,27] and femur,[28,29] which have marked differences in the trabecular characteristics compared with the maxilla and mandible.[34] Another difference compared with previous studies was the way of specimens' preparation, because most of them performed the histomorphometry on undecalcified bone specimens.[13,14,20,22,26,29]

In dental implant literature, previous studies used animal models to test the correlation or differences between microCT and histomorphometry for specific bone responses, such as the level of osseointegration based on bone-implant contact ratio[23,25] or BV.[24] However, these studies did not explore the intrinsic characteristics of the bone microstructure. Rebaudi and colleagues[8] compared microtomographic and histomorphometric analyses of peri-implant bone in a single sample from human jawbone in vivo, which revealed relevant information regarding potential of microCT, but with an obvious statistical limitation. Recently, another study[35] described the use of both methods to evaluate jawbone microarchitecture in one patient that received implant treatment. The authors emphasized the relevance of these methods to understand the bone characteristics and their influence to predict the implant success by using bone biopsies obtained during implant insertion.[35] MicroCT for human jawbone has been claimed to be validated from the earliest[18] to the most recent[25] studies that used this method in dental implant research.

Moderate to high correlation between the histomorphometric and microCT methods have been reported,[13,14,20,26–29] especially for metabolic bone diseases.[13,14,20,27,29] These studies reinforced the importance of using microCT for better characterization of bone quality as a predictor of bone strength without destroying the specimen.[2,4,13,26] In addition, microCT also provides several additional parameters that can be directly measured from the image of the bone microstructure.[4,17] However, the correlation results should be interpreted with caution because a high correlation does not automatically imply that there is good agreement between the methods,[31] as was the case for the BV/TV and BS/TV analyses performed in this study. Although BV/TV had a strong correlation between the two methods, constant bias was identified by the agreement analysis. BS/TV showed a moderate correlation, but proportional bias was observed.

In another study comparing microCT and histomorphometry, Bonnet and colleagues[22] compared the reproducibility and accuracy of two of the most widely used microCT devices (Skyscan and Scanco) with the histomorphometric method. They found high correlations between the 3D and 2D methods, except for Tb.Th (*r*-square ranging from 0.38 to 0.74), and systematic biases were found for these parameters in the Bland–Altman plots and Passing–Bablok regression. Chappard and colleagues[14] studied human transiliac biopsies and used similar methods for data analysis. Correlations between all of the parameters were highly significant, but microCT tended to overestimate BV (BV/TV), probably because of the double threshold used in microCT, showing trabecular boundaries as less well defined than the histological sections.[14] Correlations between 3D and 2D measurements were lower for Tb.Th and Tb.Sp, and 3D analysis always overestimated the thickness by approximately 50%. The authors attributed these increases to the 3D shape of the object, because the number of nodes and the size of the marrow cavities were correlated with the 3D values.[14]

Our results revealed a tendency of microCT to overestimate values for BS/TV, BS/BV, Tb.Sp, and Tb.N. A comparison of results between this study and the studies by Chappard and colleagues[14] and Bonnet and colleagues[22] must be made with caution considering the different samples that were studied, tibiae bone of female rats[22] and human iliac bone,[14] which are anatomically and structurally different from human jawbones. Additionally, it could be inferred that the difference or similarity between histomorphometric and microtomographic measurements depends on each individual parameter.[21]

Chappard and colleagues[14] as well as other authors, have warned that high correlation between histomorphometry and microCT is influenced by the threshold options[21,26,27,36] and 3D algorithm used.[20]

Determining gray scale in microCT analysis is an important step. Using different specimens (e.g., 2.7 mm/diameter × 4–13 mm/length, from different regions of the maxilla and mandible), the X-ray attenuation through the nonhomogeneous structure is not uniform, and there may exist trabeculae of varying densities that require individual selections of thresholds, as was used in this study. Skyscan microCT uses two thresholds: one when images are reconstructed from acquisition files and another one when images are binarized before morphometry. The latter is manually determined using a histogram of the pixel repartition against gray levels. Although Müller and colleagues[13] have suggested using uniform threshold, other authors have recommended proper adjustment of threshold,[22,26,36,37] because the structural indices are dependent of threshold.[38]

Demineralization technique and paraffin embedding have been used to study bone tissue, especially for pathologies diagnosis, and it is considered the standard method for immunohistochemistry and molecular evaluations.[39] However, the loss of mineralized tissue is its main disadvantage. Embedding methods using resin materials such as methyl methacrylate does not require demineralization. It has been an option for study bone tissue, especially in implantology, because it has the advantage of visualization of soft and hard tissues, as well as their relationship with another materials, including the metal of implants.[40] On the other hand, undecalcified technique is technically challenging, and besides higher cost and it being time consuming, the embedding medium can use toxic catalyst and can require deplastination prior to staining.[41] Demineralization technique/paraffin embedding was chosen based on feasibility to reuse the sample for another experiments (i.e., immunohistochemistry, molecular),[35] and because in the searched literature, no evidence that demineralization technique could significantly influence histomorphometric results was found, especially in such small sample, as was used in the present study.

Because of anisotropy of jawbone tissue, which means it has different properties in all directions, a 2D method seems to be limited to study jawbone microarchitecture and its influence on bone quality.[19] Another bias of 2D histomorphometric methods is the influence of the selection of the section plane.[16] To minimize this aspect, the most central section plane of the specimens was selected to perform the measurements, in which we expected to have the specimens' greatest dimensions. MicroCT may provide more appropriate 3D information than stereology-based histomorphometry for investigating biomechanics related to dental implants[6,19,23] and their influence on the prognosis of implant therapy.[5,6]

Based on these results, it could be concluded that histomorphometry and microCT provide complementary information regarding jawbone microarchitecture, but the poor agreement between the methods warns that their results should not be used interchangeably.

ACKNOWLEDGMENTS

We would like to thank the team involved on data collection, especially Rubelisa Cândido Gomes de Oliveira and Andrea Castro Pereira for valuable help on microtomographic and histomorphometric evaluations and EMBRAPA/CNPDIA, São Carlos, Brazil for use of the microCT scanner. This study was supported by a grant from FAPEG (Fundação de Amparo a Pesquisa do Estado de Goias, Brazil) and ILAPEO (Instituto Latino Americano de Pesquisa e Ensino Odontológico, Curitiba, Brazil), and by a scholarship from CAPES (Coordenação de Aperfeiçoamento de Pessoal de Nível Superior, Brazil, process BEX: 8436/11-8).

REFERENCES

1. Davies JE. Understanding peri-implant endosseous healing. J Dent Educ 2003; 67:932–949.
2. Ulrich D, Van Rietbergen B, Laib A, Ruegsegger P. The ability of 3D structural indices to reflect mechanical aspects of trabecular bone. Bone 1999; 25:55–60.
3. Dalle Carbonare L, Valenti MT, Bertoldo F, et al. Bone microarchitecture evaluated by histomorphometry. Micron 2005; 36:609–616.
4. Chappard D, Baslé MF, Legrand E, Audran M. Trabecular bone microarchitecture: a review. Morphologie 2008; 92:162–170.
5. Ribeiro-Rotta RF, de Oliveira RC, Dias DR, Lindh C, Leles CR. Bone tissue microarchitectural characteristics at dental implant sites part 2: correlation with bone classification and primary stability. Clin Oral Implants Res 2012. DOI: 10.1111/clr.12046.
6. Fanuscu MI, Chang TL. Three-dimensional morphometric analysis of human cadaver bone: microstructural data from maxilla and mandible. Clin Oral Implants Res 2004; 15:213–218.
7. Nkenke E, Hahn M, Weinzier lK, Radespiel-Tröger M, Neukam FW, Engelke K. Implant stability and histomorphometry: a correlation study in human cadavers

using stepped cylinder implants. Clin Oral Implants Res 2003; 14:601–609.
8. Rebaudi A, Koller B, Laib A, Trisi P. Microcomputed tomographic analysis of the peri-implant bone. Int J Periodontics Restorative and Dent 2004; 24:316–325.
9. Aksoy U, Eratalay K, Tozum TF. The possible association among bone density values, resonance frequency measurements, tactile sense, and histomorphometric evaluations of dental implant osteotomy sites: a preliminary study. Implant Dent 2009; 18:316–325.
10. Rozé J, Babu S, Saffarzadeh A, Gayet-Delacroix M, Hoornaert A, Layrolle P. Correlating implant stability to bone structure. Clin Oral Implants Res 2009; 20:1140–1145.
11. De Oliveira RCG, Leles CR, Lindh C, Ribeiro-Rotta RF. Bone tissue microarchitectural characteristics at dental implant sites. Part 1: identification of clinical-related parameters. Clin Oral Implants Res 2011; 23:981–986.
12. Parfitt AM, Drezner MK, Glorieux FH, et al. Bone histomorphometry: standardization of nomenclature, symbols and units. Report of the ASBMR histomorphometry nomenclature committee. J Bone Miner Res 1987; 2:595–610.
13. Müller R, Van Campenhout H, Van Damme B, et al. Morphometric analysis of human bone biopsies: a quantitative structural comparison of histological sections and micro-computed tomography. Bone 1998; 23:59–66.
14. Chappard D, Retailleau-Gaborit N, Legrand E, Baslé MF, Audran M. Comparison insight bone measurements by histomorphometry and micro CT. J Bone Miner Res 2005; 20:1177–1184.
15. Parfitt AM, Mathews CHE, Villanueva AR, Kleerekoper M, Frame B, Rao DS. Relationships between surface, volume, and thickness of iliac trabecular bone in aging and in osteoporosis: implications for the microanatomic and cellular mechanisms of bone loss. J Clin Invest 1983; 72:1396–1409.
16. Kopp S, Warkentin M, Öri F, Ottl P, Kundt G, Frerich B. Section plane selection influences the results of histomorphometric studies: the example of dental implants. Biomed Tech 2012; 57:365–370.
17. Chappard D, Baslé MF, Legran E, Audran M. New laboratory tools in the assessment of bone quality. Osteoporos Int 2011; 22:2225–2240.
18. Sennerby L, Wennerberg A, Pasop F. A new microtomographic technique for non-invasive evaluation of the bone structure around implants. Clin Oral Implants Res 2001; 12:91–94.
19. Moon HS, Won YY, Kim KD, et al. The three-dimensional microstructure of the trabecular bone in the mandible. Surg Radiol Anat 2004; 26:466–473.
20. Uchiyama T, Tanizawa T, Muramatsu H, Endo N, Takahashi HE, Hara T. A morphometric comparison of trabecular structure of human ilium between microcomputed tomography and conventional histomorphometry. Calcif Tissue Int 1997; 61:493–498.
21. Yeom H, Blanchard S, Kim S, Zunt S, Chu TM. Correlation between micro-computed tomography and histomorphometry for assessment of new bone formation in a calvarial experimental model. J Craniofac Surg 2008; 19:446–452.
22. Bonnet N, Laroche N, Vico L, Dolleans E, Courteix D, Benhamou CL. Assessment of trabecular bone microarchitecture by two different x-ray microcomputed tomographs: a comparative study of the rat distal tibia using Skyscan and Scanco devices. Med Phys 2009; 36:1286–1297.
23. Park YS, Yi KY, Lee IS, Jung YC. Correlation between microtomography and histomorphometry for assessment of implant osseointegration. Clin Oral Implants Res 2005; 16:156–160.
24. Schouten C, Meijer GJ, van den Beucken JJ, Spauwen PH, Jansen JA. The quantitative assessment of peri-implant bone responses using histomorphometry and micro-computed tomography. Biomaterials 2009; 30:4539–4549.
25. Vandeweghe S, Coelho PG, Vanhove C, Wennerberg A, Jimbo R. Utilizing micro-computed tomography to evaluate bone structure surrounding dental implants: a comparison with histomorphometry. J Biomed Mater Res B Appl Biomater 2013. DOI: 10.1002/jbm.b.32938.
26. Ito M, Nakamura T, Matsumoto T, Tsurusaki K, Hayashi K. Analysis of trabecular microarchitecture of human iliac bone using microcomputed tomography in patients with hip arthrosis with or without vertebral fracture. Bone 1998; 23:163–169.
27. Tamminen IS, Isaksson H, Aula AS, Honkanen E, Jurvelin JS, Kröger H. Reproducibility and agreement of micro-CT and histomorphometry in human trabecular bone with different metabolic status. J Bone Miner Metab 2011; 29:442–448.
28. Boutroy S, Vilayphiou N, Roux JP, et al. Comparison of 2D and 3D bone microarchitecture evaluation at the femoral neck, among postmenopausal women with hip fracture or hip osteoarthritis. Bone 2011; 49:1055–1061.
29. Zupan J, Van't Hof RJ, Vindišar F, et al. Osteoarthritic versus osteoporotic bone and intra-skeletal variations in normal bone: evaluation with μCT and bone histomorphometry. J Orthop Res 2013; 31:1059–1066.
30. Brånemark P-I, Zarb GA, Albrektsson T. Tissue-integrated prostheses: osseointegration in clinical dentistry. 1st ed. Chicago, IL: Quintessence, 1985:199–209.
31. Bland JM, Altman DG. Statistical methods for assessing agreement between two methods of clinical measurement. Lancet 1986; 1:307–310.
32. Krouwer JS, Monti KL. A simple, graphical method to evaluate laboratory assays. Eur J Clin Chem Clin Biochem 1995; 33:525–527.

33. Passing H, Bablok W. A new biometrical procedure for testing the equality of measurements from two different analytical methods. Application of linear regression procedures for method comparison studies in clinical chemistry, Part I. J Clin Chem Clin Biochem 1983; 21:709–720.
34. Bodic F, Amouriq Y, Gayet-Delacroix M, et al. Relationships between bone mass and micro-architecture at the mandible and iliac bone in edentulous subjects: a dual X-ray absorptiometry, computerised tomography and microcomputed tomography study. Gerodontology 2012; 29:585–594.
35. Yamashita-Mikami E, Tanaka M, Sakurai N, et al. Microstructural observation with microCT and histological analysis of human alveolar bone biopsy from a planned implant sity: a case report. Open Dent J 2013; 7:47–54.
36. Chang PC, Liang K, Lim JC, Chung MC, Chien LY. A comparison of the thresholding strategies of micro-CT for periodontal bone loss: a pilot study. Dentomaxillofac Radiol 2013; 42:66925194. DOI: 10.1259/dmfr/66925194.
37. Feldkamp LA, Goldstein SA, Parfitt AM, Jesion G, Kleerekoper M. The direct examination of three-dimensional bone architecture in vitro by computed tomography. J Bone Miner Res 1989; 4:3–11.
38. Rüegsegger P, Koller B, Müller R. A microtomographic system for the nondestructive evaluation of bone architecture. Calcif Tissue Int 1996; 58:24–29.
39. Yang R, Davies CM, Archer CW, Richards RG. Immunohistochemistry of matrix markers in Technovit 9100 New-embedded undecalcified bone sections. Eur Cell Mater 2003; 6:57–71.
40. Donath K, Breuner G. A method for the study of undecalcified bones and teeth with attached soft tissues. The Säge-Schliff (sawing and grinding) technique. J Oral Pathol 1982; 4:318–326.
41. Quester R, Knifka J, Schröder R. Optimization of glycol methacrylate embedding of large specimens in neurological research. Study of rat skull-brain specimens after implantation of polyester meshes. J Neurosci Methods 2002; 113:15–26.